

On the Control of Soil Heterogeneity, Peclet number and Spatially Variable Diffusion over Unsaturated Transport

Christopher V. Henri¹, Efstathios Diamantopoulos²

¹Geological Survey of Denmark and Greenland, Copenhagen, Denmark

²Chair of Soil Physics, University of Bayreuth, Bayreuth, Germany

Key Points:

- Small scale soil heterogeneity has a significant Peclet number dependent impact on main transport characteristics.
- Diffusion can have a profound impact on transport, which is dependent on soil heterogeneity and the Peclet number.
- The spatial variability in the diffusion coefficient significantly controls transport, but remains complex to upscale.

Abstract

Physical properties of soils are ubiquitously heterogeneous. This spatial variability has a profound, yet still partially understood, impact on conservative transport. Moreover, molecular diffusion is often a disregarded process that can have an important counter-intuitive effect on transport: diffusion can prevent non-Fickian tailing by mobilizing mass otherwise trapped in low velocity zones. Here, we focus on macroscopically homogeneous soils presenting small scale heterogeneity, as described by the Miller-Miller method. We then analyze the dynamic control of soil heterogeneity, advection and diffusion on conservative transport. We focus especially on the importance of diffusion and of its tortuosity-dependent spatial variability on the overall transport. Our results indicate that high Peclet number systems are highly sensitive to the degree of heterogeneity, which promotes non-Fickian transport. Also, diffusion appears to have a profound impact on transport, depending on both the degree of heterogeneity and the Peclet number. For a high Peclet number and a very heterogeneous system, diffusion leads to the counter-intuitive decrease of non-Fickian macrodispersion described previously. This is not observed for a low Peclet number due to the non-trivial impact of the spatial variability in the diffusion coefficient, which appears to be a significant controlling factor of transport by promoting or preventing the accumulation of mass in low velocity zones. Globally, this work (1) highlights the complex, synergistic effect of soil heterogeneity, advective fluxes and diffusion on transport and (2), alerts on potential upscaling challenges when the spatial variability of such key processes cannot be properly described.

1 Introduction

Understanding and predicting the dynamics of chemicals in soils is key to optimize agrochemical application while ensuring the protection of the water resources. However, the fate of chemicals in soils results from a complex interplay of physical, chemical and biological processes which are still not well understood. For a non-reactive, non-sorbing and non-volatile conservative solute, it is well established that the main physical processes controlling transport are advection, diffusion and dispersion (Bear, 1972). Thus, the advection-dispersion-diffusion equation (ADE), which mathematically describes those processes at the continuum scale (Cushman, 1984), represents to this day the most popular theory describing solute transport into porous media. Yet, the parameters in the

ADE are effective parameters, integrating small scale spatial variability in the physical properties of soils, which often challenges its application.

Soils are heterogeneous at any spatial scale, from the pore scale (mm) up to the catchment scale (km). Soil heterogeneity can result from diverse origins such as parent material, pedogenesis, soil organisms, plant roots and anthropogenic impact like management operations (Schelle et al., 2013). Soil heterogeneity is intrinsically spatial scale dependent and it may include spatial variability of different properties. A heterogeneous soil can for example originate from different soil textures observed at relatively large scales ($> \text{dm}$, e.g., soil horizons), and/or from different arrangements of the same mineral grains at smaller spatial scales (cm). Some components can also span different spatial scales like macropores from earthworms, roots, etc (Jarvis et al., 2016; Holbak et al., 2022). In any ways, the variability in physical properties provokes variability in soil hydraulic properties (SHPs), subsequently leading to dynamic hydraulic structures (Javaux et al., 2006a) exposing, e.g., a complex network of high flux channels with interspersed small volumes of low-flux domains (Roth, 1995).

The spatial variability of the physical properties of soils has a substantial effect on transport of conservative solutes, which has been extensively reported since the 1990's (e.g., Roth, 1995; Hammel & Roth, 1998; Javaux et al., 2006b; Russo & Fiori, 2009; C. J. M. Cremer & Neuweiler, 2019, among many others). Understanding this effect of heterogeneity on transport dynamics is key to accurately estimate and predict solute transport toward the water resources (Russo, 2015) and to develop useful upscaling techniques (e.g., dual-permeability approach, Vogel et al., 2000). Unsaturated heterogeneous transport has been experimentally observed under laboratory (Khan & Jury, 1990), large soil monoliths (Javaux et al., 2006b) and field conditions (Forrer et al., 1999; Ursino & Gimmi, 2004). Yet, the vast complexity of unsaturated systems has often led researchers to study the transport of conservative solutes in saturated/unsaturated porous media through numerical experiments. In most of those studies, soil heterogeneity has been explicitly represented at the cm scale (Roth & Hammel, 1996), assuming the validity of a similarity model for the small scale SHPs, as done by, e.g., the Miller-Miller Similar Media Theory (MMT) (Miller & Miller, 1956; Sadeghi et al., 2016).

Results from such studies show that the impact of heterogeneity on transport appears to not be a well defined soil dependent feature, but results instead from the syn-

ergistic effect of constitutive material spatial variability and of dynamic flow conditions. For instance, decreasing the degree of saturation will increase the spread of the solute (Russo, 1993) and the effective recharge rate (i.e. vertical flux) controls more specifically the transverse dispersion (Roth & Hammel, 1996; Hammel & Roth, 1998; Forrer et al., 1999; Cirpka & Kitanidis, 2002). Thus, considering more realistic conditions in terms of contaminant input fluxes (Vanderborght et al., 1998), flow dynamic characterized by infiltration (downward fluxes)-evaporation (upward fluxes) periods (Russo et al., 2000, 2001; C. J. Cremer et al., 2016; Henri & Diamantopoulos, 2022), or topography (Woods et al., 2013) results to even more complex transport behavior, which remains to this day challenging to systematically describe.

Despite an improved understanding of heterogeneous transport in soils, to this day, even models considering some type of heterogeneity generally fail to predict observed plume behavior, in terms of travel times and spread (Ursino & Gimmi, 2004), scale and flow rate dependency of transport (Javaux et al., 2006b), and contaminant concentrations (Botros et al., 2012). While it is a common knowledge that applying the ADE or any of its extension (e.g., Mobile-Immobile theory (Van Genuchten & Wierenga, 1974)) can successfully describe experimental data under different spatial scales, the predicting capabilities of those theories remain indeed limited, which highlight the complexity to fully represent the variety of processes engaged in the subsurface.

In this context, it is worth mentioning that, although molecular diffusion is a process that is sometimes accounted for in numerical experiments (C. J. Cremer et al., 2016), its effect on transport is often disregarded. Nevertheless, some theoretical studies have highlighted diffusive transport as a potentially important process controlling factor of solute behavior under both unsaturated and saturated conditions (Weissmann et al., 2002; Nissan & Berkowitz, 2019; Cirpka & Kitanidis, 2002).

The importance of diffusion is in most cases studied relatively to advection. The Peclet number (Pe), comparing advective and diffusive characteristic times, is then the reference metric to characterize dominance of either process to the overall transport. Importantly, it has been shown that the Peclet number controls the effect of heterogeneity on solute transport. This observation has been made at different spatial scales and in both saturated and unsaturated conditions. For instance, studies by Nissan & Berkowitz (2019) at the (saturated) pore scale, Cirpka & Kitanidis (2002) at the (unsaturated) site

scale and (Weissmann et al., 2002) in a regional aquifer show that high Pe values (i.e., a predominance of advection over diffusion) leads to more anomalous behavior compared to low Pe values. Inversely, transport at low Pe (i.e., diffusion-dominant) is characterized by shorter residence times in stagnant zones, which reduces the anomalous behavior of transport. In simple terms, a strong diffusion reduces the “delay” in very low velocity zones of the porous medium by favoring the transfer of solute mass from these quasi-stagnant areas to more mobile ones. It has been also shown at the pore scale and under saturated conditions that this sensitivity of transport to Pe is accentuated by increasing the degree of heterogeneity in the porous media (Nissan & Berkowitz, 2019). Such transport dynamic remains to be confirmed at larger scale and under unsaturated conditions.

From the previous, it is obvious that the effect of molecular diffusion on transport is well documented, but the process is in most cases represented as being uniform (i.e., described by a constant diffusion coefficient). Yet, it is also well documented that in any porous system, the presence of solid-air-liquid interfaces influences the diffusion paths of solute species (Boudreau, 1996). The effect of water content/porosity on the effective diffusive process is often represented as a dependence of the diffusion coefficient to tortuosity (Shen & Chen, 2007; Ghanbarian et al., 2013; Van Cappellen & Gaillard, 2018). In unsaturated soils, spatial and temporal variability in the water content can then make the diffusion process highly heterogeneous. Yet, rare are the studies that have explicitly analyzed the effect of a tortuosity-dependency of the diffusion coefficient, especially under heterogeneous conditions. For instance, C. J. Cremer et al. (2016) uses the Millington & Quirk (1961) method to account for tortuosity but the authors do not assess the relevance or the importance of such approach on diffusive transport.

This study aims on the understanding of conservative transport in unsaturated soils, and more specifically on the complex interplay between spatial heterogeneity of SHPs, advection and diffusion. As mentioned above, real soils are structured at many different scales (horizons, macropores, anisotropy, etc) and these components are expected to add additional complexity to water flow. In this study, we focused solely on the effect of small scale heterogeneity and its impact on transport, similar to the studies of Roth & Hammel (1996) and Hammel & Roth (1998). After analyzing the complex synergistic control of soil heterogeneity and infiltration flux, we will focus more specifically on

the superposed impact of diffusion and of its spatial variability on heterogeneous transport.

2 Method

In the following, we briefly present the theory for i) simulating water flow and conservative transport in unsaturated soils, ii) representing heterogeneity with MMT, and finally, iii) we provide an overview of all the tested numerical experiments.

2.1 Flow and transport

Flow. For a rigid, non-swelling, isotropic porous medium, water flow under variable saturated conditions is described by the Richards-Richardson equation (Richards, 1931; Richardson, 1922):

$$\frac{\partial \theta}{\partial t} = -\nabla \cdot \theta \mathbf{u} = \nabla \cdot [K \nabla h] + \frac{\partial K}{\partial z} \quad (1)$$

where z is the vertical coordinate [L], h is the pressure head [L], θ is the volumetric water content [$\text{L}^3 \text{L}^{-3}$], \mathbf{u} is the pore water velocity [L T^{-1}] and K [L T^{-1}] is the saturated/unsaturated conductivity as a function of θ or h . A prerequisite of Equation 1 is that the air pressure in the soil at any system state is equal to the atmospheric pressure (single flow).

Eq. 1 assumes that, at the continuum scale (Cushman, 1984), a local equilibrium between water content and pressure head is always valid (Diamantopoulos & Durner, 2012). This relationship is described by the water retention curve:

$$h(S_e) = \frac{1}{\alpha} [S_e^{-n/(n-1)} - 1]^{(1/n)}, \quad (2)$$

where S_e [-] is the effective saturation given by:

$$S_e(\theta) = \frac{\theta - \theta_r}{\theta_s - \theta_r}, \quad (3)$$

and α [L^{-1}] and n [-] are shape parameters. θ_s [$\text{L}^3 \text{L}^{-3}$] and θ_r [$\text{L}^3 \text{L}^{-3}$] are saturated and residual water contents. Finally, the conductivity as a function of effective saturation is given by:

$$K(S_e) = K_s S_e^\tau [1 - (1 - S_e^{n/(n-1)})^{1-1/n}]^2 \quad (4)$$

For all the simulations presented in this work, we assumed a simulation domain of 80 cm in the horizontal direction (L_x) and 240 cm in the vertical direction (L_z). The domain was discretized in cells of size $d_x = 1$ cm and $d_z = 2$ cm, respectively, resulting in $n_x = 80$ numerical nodes in the x-direction and $n_z = 120$ in the z-direction. The length of the domain was chosen to ensure 10 correlation lengths in each direction in order to capture the full (i.e., ergodic) effect of heterogeneity (presented below in paragraph 2.2). At the top nodes ($z=0$ cm), a constant flux boundary condition was chosen, whereas at the bottom ($z=240$ cm) a unit-hydraulic head gradient was assumed. For the numerical solution of Eq. 1, the finite-volume method as implemented in the Daisy model (Hansen et al., 2012; Holbak et al., 2021) has been used.

Transport. Transport in the unsaturated zone for a conservative solute is described by the advection-dispersion equation:

$$\frac{\partial(\theta c)}{\partial t} = -\nabla \cdot (\theta \mathbf{u} c) + \nabla \cdot (\theta \mathbf{D} \cdot \nabla c), \quad (5)$$

where c [M L^{-3}] is the solute concentration, θ [$\text{L}^3 \text{L}^{-3}$] is the water content and \mathbf{D}^w [$\text{L}^2 \text{T}^{-1}$] is the hydrodynamic dispersion tensor in the water phase given by (Bear, 1972):

$$\mathbf{D} = (\alpha_T |\mathbf{u}| + D_m) \delta + (\alpha_L - \alpha_T) \frac{\mathbf{u} \mathbf{u}^T}{|\mathbf{u}|}, \quad (6)$$

where α_L [L] and α_T [L] is the longitudinal and transverse dispersivities, respectively, D_m [$\text{L}^2 \text{T}^{-1}$] is the molecular diffusion and δ is the Kronecker delta function.

The ADE was solved using the Random Walk Particle Tracking (RWPT) method, expressed as:

$$\mathbf{x}_p(t + \Delta t) = \mathbf{x}_p(t) + \mathbf{A}(\mathbf{x}_p, t) \Delta t + \mathbf{B}(\mathbf{x}_p, t) \cdot \xi(t) \sqrt{\Delta t}, \quad (7)$$

where \mathbf{x}_p is the particle location, Δt is the time step of the particles jump and ξ is a vector of independent, normally distributed random variables with zero mean and unit variance.

$$\mathbf{A} = \mathbf{u}(\mathbf{x}_p) + \nabla \cdot \mathbf{D}(\mathbf{x}_p) + \frac{1}{\theta(\mathbf{x}_p)} \mathbf{D}(\mathbf{x}_p) \cdot \nabla \theta(\mathbf{x}_p). \quad (8)$$

The displacement matrix relates to the dispersion tensor as:

$$2\mathbf{D} = \mathbf{B} \cdot \mathbf{B}^T. \quad (9)$$

The RWPT approach, implemented in the code RW3D (Fernández-García et al., 2005; Henri & Fernández-García, 2014, 2015), is further described for application in unsaturated conditions by Henri & Diamantopoulos (2022), who also shows how the Lagrangian method avoids numerical issues typically produced by Eulerian schemes.

Diffusion. The effective diffusion coefficient (D_m) was considered to be dependent on the local water content value (Shen & Chen, 2007):

$$D_m(\theta) = D_w \times \tau_w(\theta), \quad (10)$$

where D_w [$\text{L}^2 \text{T}^{-1}$] is the diffusion coefficient in free water, and $\tau_w(\theta)$ is the water content dependent tortuosity. $\tau_w(\theta)$ is typically described empirically. Different models are frequently used, and in this study the relationship described by Millington & Quirk (1961) was used:

$$\tau_w(\theta) = \frac{\theta^{7/3}}{\theta_s^2}. \quad (11)$$

For comparison, we also consider the relationship proposed by Møldrup et al. (1997):

$$\tau_w(\theta) = 0.66 \times \left(\frac{\theta}{\theta_s} \right)^{8/3}. \quad (12)$$

The Millington & Quirk (1961) tortuosity model is expected to perform better for sands, since it was derived assuming randomly distributed particles of equal size. On the other hand, the tortuosity model proposed by Møldrup et al. (1997) is expected to perform better across soil types (Šimunek et al., 2013).

For each simulation, 10^5 particles were injected randomly over a transect of 40 cm located at the center of the top of the domain. To avoid potential subsampling due to particles leaving the sides of the domain, a semi-infinite width was considered by transferring particles leaving the domain at $x=0$ and $x=L_x$ to the other side of the domain, at $x=L_x$ and $x=0$, respectively. The impact of such approximation, previously used by, e.g., Cirpka & Kitanidis (2002), appears to be minor on both apparent velocity and dispersion, and does not therefore affect our conclusions (see Supplementary Information, Figure S1).

The time step between particle jumps was defined to preserve the advective displacement, which was done using a grid Courant number (gCu) as:

$$\Delta t = gCu \times \Delta s / \min\{u_x, u_y, u_z\}, \quad (13)$$

Table 1. Hydraulic properties of the reference material used for all simulations: saturated (θ_s) and residual (θ_r) water contents, shape parameters (α , n), saturated hydraulic conductivity (K_s).

Material	θ_r [cm ³ cm ⁻³]	θ_s [cm ³ cm ⁻³]	α [cm ⁻¹]	n [-]	K_s [cm h ⁻¹]
Loam	0.00	0.49	0.0066	1.68	1.8

where Δs is the characteristic size of the grid cell.

2.2 Representation of soil heterogeneity

Small scale soil heterogeneity was modeled using the MMT method (Miller & Miller, 1956; Sadeghi et al., 2016). Briefly, the theory assumes that similarities at the pore scale geometry yields characteristic length or scaling factors (ζ), which scale the physical properties of porous media, in this case the water retention and hydraulic conductivity curve (Roth & Hammel, 1996; Schelle et al., 2013; Sadeghi et al., 2016). For each location \mathbf{x} , we can then calculate location-dependent soil hydraulic properties by:

$$h(\mathbf{x}, \theta) = h^*(\theta) \frac{1}{\zeta(\mathbf{x})}, \quad (14)$$

$$K(\mathbf{x}, \theta) = K^*(\theta) \zeta(\mathbf{x})^2, \quad (15)$$

where $h^*(\theta)$ and $K^*(\theta)$ are reference material properties, described in Eq. 2 and Eq. 4. Detailed theoretical considerations for MMT along with an overview of theory applications is provided in Sadeghi et al. (2016). For all simulations, we assumed a single loam material and the parameters of Eq. 2-4 are provided in Table 1. The spatial distribution of the log-scaling factor $\chi \equiv \log_{10}(\zeta)$ (presented above) was geostatistically described as a multi-Gaussian model characterized by an isotropic Gaussian covariance function with zero mean and a standard deviation σ_χ . Different σ_χ values have been tested in this study. Finally, the correlation length in x (λ_x) and z (λ_z) was fixed to 8 cm and 24 cm, respectively, following the work of Schlüter et al. (2012).

The Miller-Miller theory assumes that porosity, and thus water content at saturation (θ_s), is constant (through out this work equal to 0.49 cm³cm⁻³, Table 1). To test

the implications of spatial distributed θ_s , we also ran a set of simulations scaling θ_s linearly as a function of the local K_s value, with a minimum and maximum value of 0.3 and 0.6, respectively. In that way, the test simulations assumed that high values of θ_s coincide with high values of K_s . This was only done for a high heterogeneity and a low mean velocity ($\sigma_\chi = 0.5$ and $q = 0.01$ mm/h, diffusion dominated process), which represent the scenario most likely to be affected by an assumed constant θ_s .

2.3 Tested scenarios

Water flow was simulated for a series of steady-state simulations, assuming three different degrees of heterogeneity ($\sigma_\chi = 0.1, 0.3, 0.5$) and two different imposed vertical water fluxes ($q_{z,in} = 0.01, 1$ mm/h), and thus, different hydraulic structures (Table 2). The low flux represents a scenario strongly dominated by diffusion (low mean velocity), whereas the high flux represents a scenario with a stronger advective component, as observed during an infiltration period. For each combination of σ_χ and $q_{z,in}$, 20 realizations have been created. While this limited number of realization is not likely to be sufficient for a stochastic analysis, observing results from a series of equiprobable flow fields will allow to determine if our observation are realization specific or systematic.

For all the water flow simulations, solute transport was also simulated. The non-represented effect of heterogeneity within a grid cell was accounted for by setting a grid-scale dispersivity values of 0.1 cm in the longitudinal direction (i.e., z), and 0.01 cm in the transverse direction (i.e., x). Moreover, D_w was fixed to $1.6 \text{ cm}^2/\text{d}$ (order of magnitude similar to, e.g., C. J. Cremer et al. (2016)). To better understand the implications of a spatially variable diffusion process, we tested 2 different methods on simulating the diffusion coefficient (Table 2):

- A spatially variable, tortuosity (i.e., water content) dependent diffusion coefficient ($D_m(\mathbf{x})$), with a tortuosity model described by (Millington & Quirk, 1961), as described in Eq. 11;
- A spatially averaged diffusion coefficient (\bar{D}_m).

The diffusion coefficient was considered to be the same values in the x and z direction.

Finally, we evaluated the effect of transient conditions on solute transport in a highly heterogeneous soil ($\sigma_\chi = 0.5$, Table 2). Transient conditions are caused by an infiltra-

Table 2. Tested scenarios.

Description	Heterogeneity	Water flow	Diffusion
Steady state simulations (20 realizations)	$\sigma_\chi = 0.1$	$q_{z,in} = 0.01$ mm/h	Constant, averaged (\bar{D}_m)
	$\sigma_\chi = 0.3$	$q_{z,in} = 1$ mm/h	Tortuosity dependent ($D_m(x)$)
	$\sigma_\chi = 0.5$		
Transient simulations (1 realization)	$\sigma_\chi = 0.5$	1 day of strong infiltration	Constant, averaged (\bar{D}_m)
		15 days of strong infiltration	Tortuosity dependent ($D_m(x)$)

tion period followed by a long redistribution period. Two different infiltration periods (t_{inf}) are considered: 1 and 15 days. The two models of diffusion tested for the steady state simulations are here also considered.

3 Results

3.1 Small scale soil heterogeneity and advective flux

In this section, we analyze simulation results of a single realization. Nevertheless, we also present outputs from the ensemble of 20 realizations in term of arrival time statistics to ensure that observations made on a single realization are consistent across realization.

Flow fields. Throughout our analysis, the intensity of the advective flux is characterized by the Peclet number (Pe), which is estimated as:

$$Pe = \frac{\bar{u}_z \lambda_z}{\bar{D}_m}. \quad (16)$$

where \bar{u}_z [$L T^{-1}$] is the average pore water velocity in the z direction.

The resulting Peclet numbers, for each degree of heterogeneity, was equal to 3.3×10^{-1} , 3.3×10^{-1} , 3.4×10^{-1} , respectively, for the high flux; and equal to 4.0×10^{-2} , 2.9×10^{-2} , 1.9×10^{-2} , respectively, for the low flux. According to the calculated Peclet numbers, all scenarios are diffusion dominated ($Pe < 1$). However, the low $q_{z,in}$ simulations can be characterised as strongly dominated by diffusion, due to the one order of magnitude lower Peclet number.

The spatial variability of SHPs appears to significantly control both saturation and local water fluxes. Clear patterns of quasi-dry ($\theta < 0.1$) and near-saturated ($\theta \approx \theta_s$) zones emerges when the degree of heterogeneity is increased (Figure 1, left frames; results from the lower degree of heterogeneity are shown in Supplementary Information, Figure S2 and Figure S3).

The spatial variability in saturation is also highly sensitive to the intensity of the infiltration flux (Figure 1, compare upper and lower left frames). Globally, saturation is logically increased in case of higher Pe . Moreover, the degree of heterogeneity in computed θ in case of high σ_χ appears to decrease when infiltration is stronger. We indeed observe an increased predominance of fully saturated areas ($\theta \approx \theta_s$), which is a direct effect of MMT and the inherent assumption of equal saturated water content.

Similar observation can be made while analyzing the combined effect of soil heterogeneity and input flux on the spatial variability of computed water (Darcian) fluxes (Figure 1, middle frame) and pore velocities (Figure 1, right frame): (1) Increasing σ_χ generates clear zones of low velocity and fast paths, and (2) increasing the infiltration flux globally increases fluxes and increase the portion of the soil column occupied by high velocity zones. These results are globally consistent with past work such that of Roth (1995), who also observed the clear formation of islands of low and high fluxes due to a similar Miller-Miller heterogeneous media and the sensitivity of this hydraulic structure to the input flux.

Spatial moments. The effect of heterogeneity and infiltration flux on the dynamic hydraulic structure is reflected on the transport behavior of the applied particles. We first analyze the lower spatial moments of the plume: the first moment, z_g , represents the location of the center of mass, and the second spatial moment, S_{zz} , quantifies the spread around the centroid of the plume.

Spatial moments are evaluated until particles start to leave the downstream edge of the domain to reflect the dynamics of the entire plume. Only results from simulations using the “Millington and Quirk” model of tortuosity is shown throughout our analysis. The analysis using the “Moldrup et al.” model leads to similar results as shown in Supplementary Information, Figure S4.

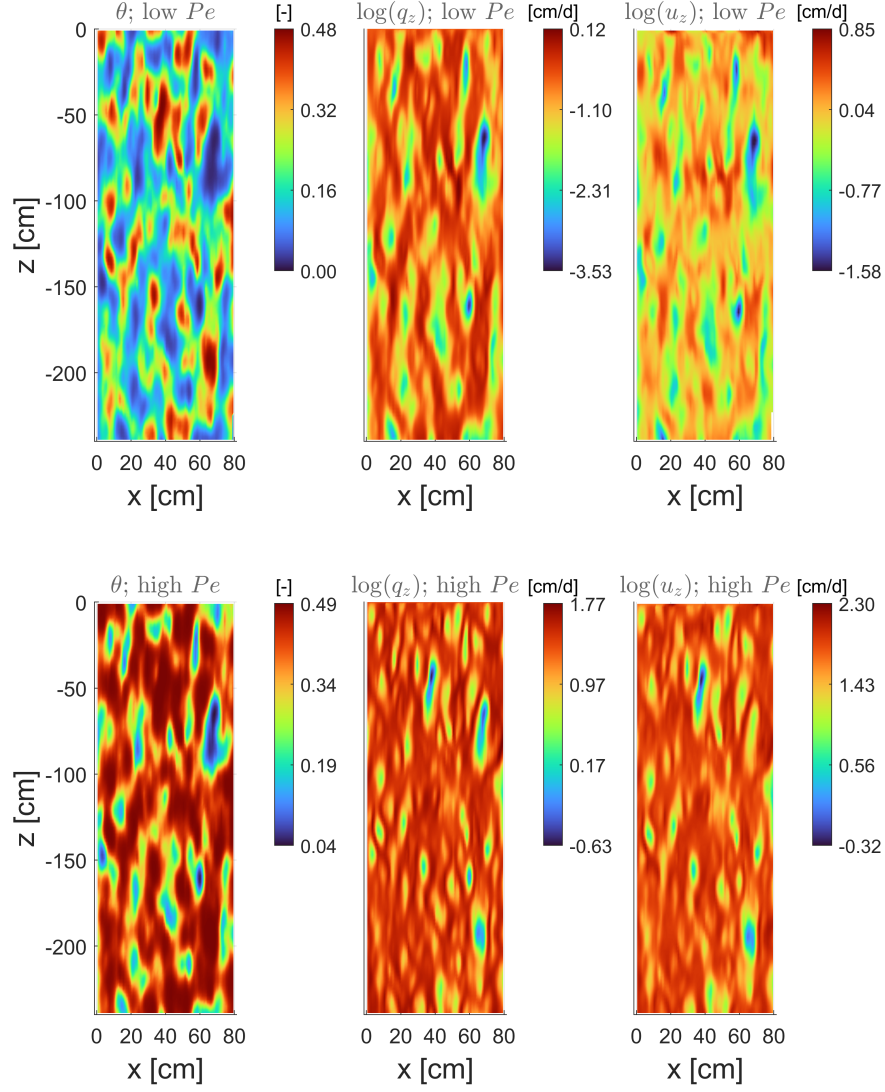


Figure 1. Resulting spatial distribution of the water content (θ) for the highest degree of soil heterogeneity ($\sigma_\chi = 0.5$) and for a high recharge flux (i.e., high Peclet number; bottom frames) and a low recharge flux (i.e., low Peclet number; top frames).

The center of mass of the plume is highly sensitive to the degree of heterogeneity in SHPs for the case of low Pe number (Figure 2). For the same infiltration flux, the plume moves downward faster in case of low σ_χ (Figure 2, top left frame). The effective velocities in the downward direction associated to each σ_χ values, v_z^* , can be quantified as the slope of the linear regression of $z_g(t)$, giving: 0.12, 0.08 and 0.05 cm/d for the low input flux scenario, respectively, and 6.1, 6.0, 5.2 cm/d for the high input flux scenario. Characteristic advection times can then be estimated as: $t_{adv} = L_z/v_z^*$.

Interestingly, the temporal evolution of the first spatial moment observed for the low Pe case presents a non-linearity that increases with σ_χ . This results to periods of acceleration and of slowing down of the center of mass of the plume and not to a constant effective velocity as observed in case of $\sigma_\chi=0.1$. The sensitivity of the effective velocity to the degree of heterogeneity is lower in case of high Pe (Figure 2, top right frame). This non-linearity appears to be more or less pronounced depending on the realizations (Supplementary Information, Figure S5).

The spread of the plume appears to be less sensitive to σ_χ in case of a low Pe than in case of a high Pe (Figure 2, compare bottom frames). For a high Pe , the spread is significantly increased for the highest degree of heterogeneity. For the low Pe , a low input flux applied on a highly heterogeneous media leads to different regimes of spread of the plume, with an intensification of the spread at early and intermediate times (Figure 2, bottom left frame). These fluctuations are observed for most realizations (Supplementary Information, Figure S6). Yet, the average magnitude of the spread remains globally similar for all σ_χ , unlike for a high Pe .

Breakthrough curves. Such observations have clear implications in term of mass transfer from the soil to deeper layers and into the aquifer. When heterogeneity is increased in a low velocity system, the breakthrough curve recorded at the bottom of the simulated domain presents a later mass arrival and an increased spread, i.e., lower peak of mass and mass arrival for a longer period (Figure 3, top left frame). Distinctively, early mass arrival appears insensitive to the degree of heterogeneity in case of high input flux, unlike macrodispersion, which sensitively increases with σ_χ (Figure 3, bottom left frame).

Globally, those results are consistent with the direct observation of non-Fickian transport in macroscopically homogeneous unsaturated media with similar high velocity (Bromly & Hinz, 2004).

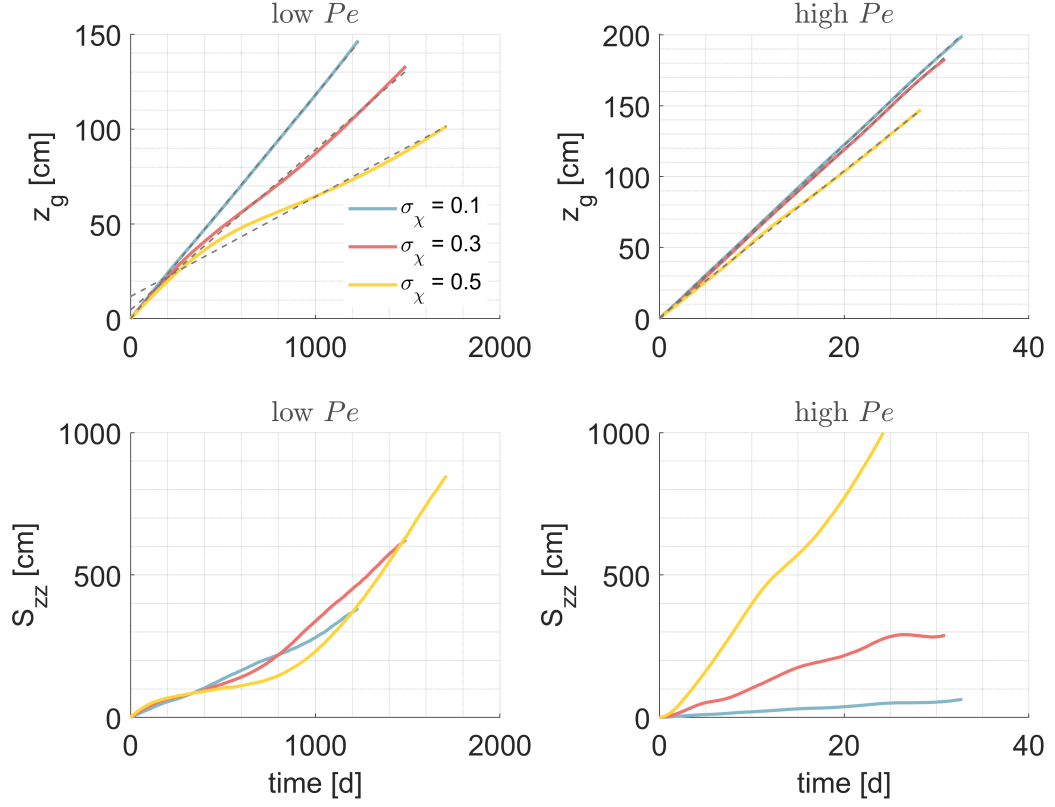


Figure 2. First (center of mass location, z_g ; top frames) and second (spread about the centroid, S_{zz} ; bottom frames) normalized spatial moments for each degree of heterogeneity of the soil structure and for the 2 input fluxes. The dashed grey lines on the top frames are linear regressions for the temporal evolution of z_g . The slopes of the regression represent effective velocities.

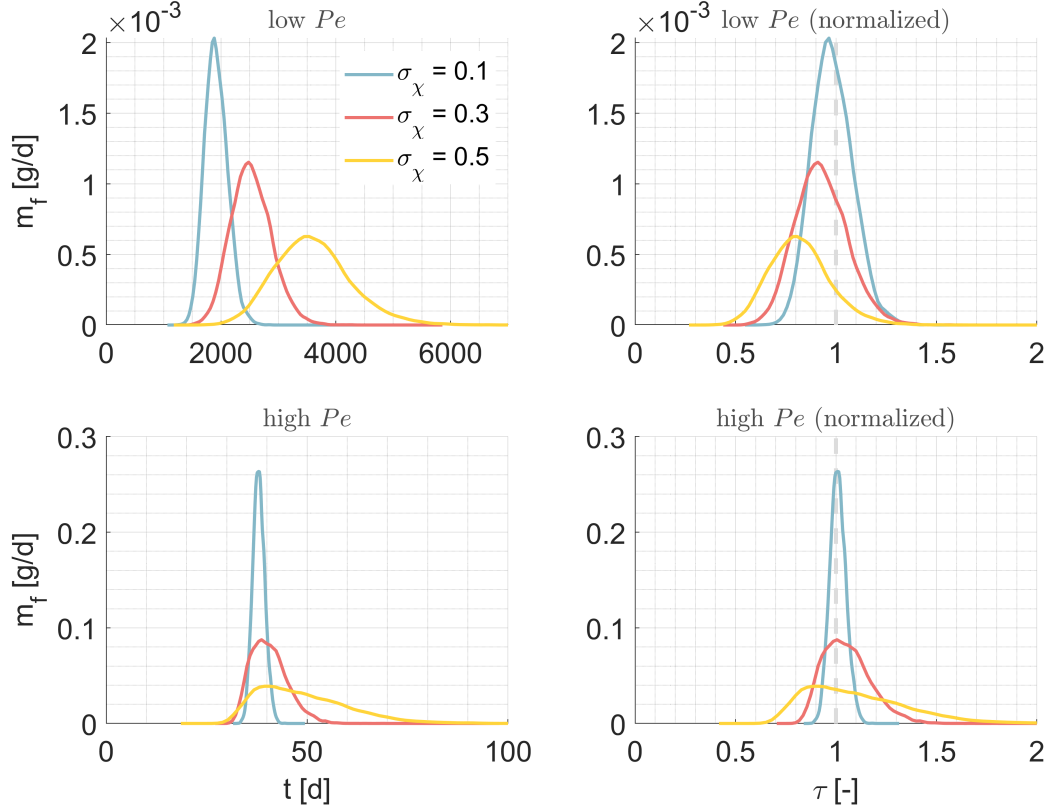


Figure 3. Breakthrough curves (BTCs) resulting from simulations in soil of different degree of heterogeneity, for a high recharge flux (i.e., high Peclet number; bottom frames) and a low recharge flux (i.e., low Peclet number; top frames). Right frames show the BTCs considering a time normalized by the advective time. The diffusion coefficient is considered spatially variable (tortuosity dependent).

Observing the plume behavior in a series of 20 realization of the heterogeneity in the SHPs is consistent with the analysis made on single BTCs. For the high Pe system, early arrival times (t_5) are less sensitive to σ_χ than late arrival times (t_{95} ; Supplementary Information, Figure S7, left frames), while all arrival times are increased with heterogeneity when Pe is lower (Figure S7, right frames). Also, travel times *pdfs* allow to observe that the variability among realizations in late arrival times is significantly increased with the degree of heterogeneity.

The first spatial moment is often used to subsequently estimate the effective velocity (v_z^*) and the time of arrival of the center of mass of the plume at *any* distance from the source. Applying this approach is valid in case of high input flux (Figure 3, bottom

right frame). The BTCs are centered around a unit values of time normalized by t_{adv} , regardless of the degree of heterogeneity. However, we observe that v_z^* does not properly predict the motion of the plume in case of low flux and high σ_χ (Figure 3, top right frame). Normalizing the BTCs' time by the characteristic advective time (t_{adv}) leads to faster first arrival of mass for low Pe and high σ_χ systems, reflecting an overall overestimation of the effective velocity.

This results from the non-linear behavior of the first spatial moment observed in soils characterized by a low Pe and a high σ_χ (Figure 2). Indeed, the predictive capacities of the first spatial moment implies a linear evolution of the center of mass location, reflecting a constant effective velocity, which is often observed in saturated conditions. $t = t_{adv}$ would then be associated to the arrival of the center of the plume at the characteristic distance used to estimated t_{adv} (L_z in our case). Yet, in case of low flux, the center of mass of the plume is affected by critical moments of fast and slow motion, which render more complex the estimation of an effective behavior.

3.2 Importance of diffusion

In this section, our analysis focuses on the effect of diffusion on transport. We first analyze the relevance of considering a realistically heterogeneous diffusion coefficient ($D_m(x)$, blue curves in Figures 4 and 5) by comparing corresponding BTCs from simulations disregarding the diffusive process (yellow lines). The implications of considering a spatially homogeneous diffusion coefficient (\bar{D}_m) will be analyzed in the following section.

High Peclet number. For a high Pe , considering diffusion has a moderate effect on macrodispersion. In case of low heterogeneity, disregarding diffusion all together decreases macrodispersion (Figure 4), which is the expected expression of the process. Increasing σ_χ renders more complex the impact of diffusion on transport: Early arrival times are mostly unchanged but macrodispersion is decreased by adding diffusion, decreasing the very pronounced tailing (i.e., elongated late arrivals) generated by the heterogeneity in the advective flux. This phenomena has been previously observed by few studies under various conditions (Nissan & Berkowitz, 2019; Cirpka & Kitanidis, 2002; Weissmann et al., 2002) and is explained by the capacity of diffusive motion to move mass away from quasi-stagnant zones, reducing this way the potential for very late arrivals (i.e., tail-

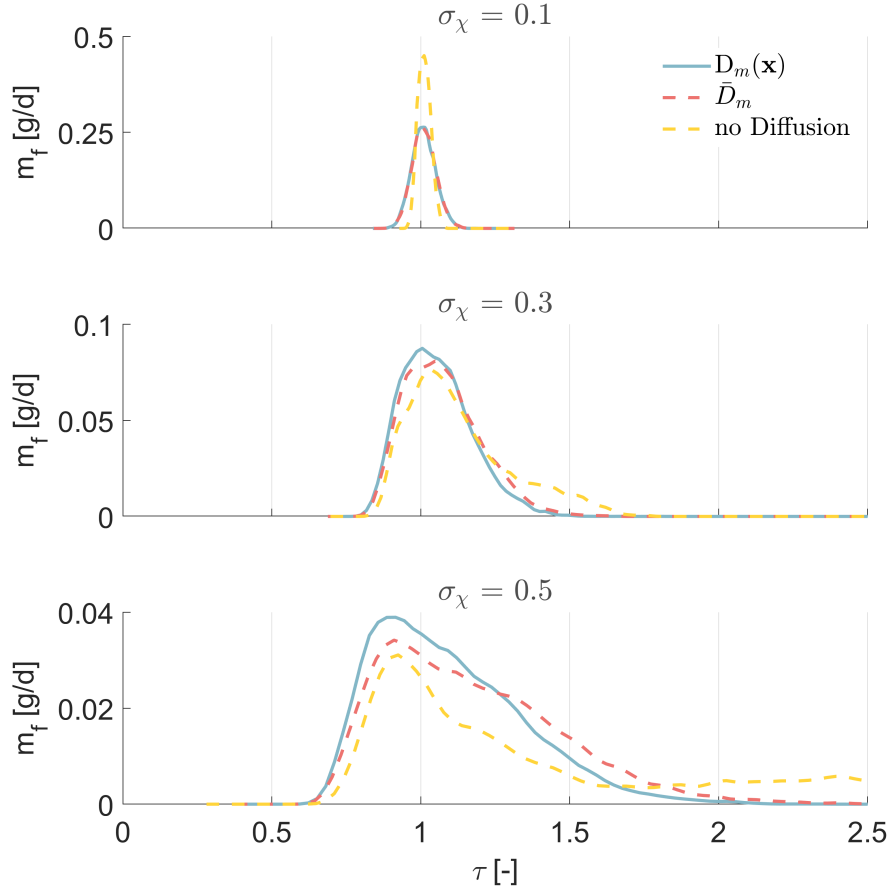


Figure 4. Breakthrough curves (BTCs) resulting from simulations using a spatially variable, tortuosity-dependent diffusion coefficient ($D_m(x)$) and a spatially averaged diffusion coefficient (\bar{D}_m) and no diffusion, for soils of different degree of heterogeneity. Results are shown for the higher Peclet number. Times are normalized by the characteristic advective time of the $D_m(x)$ scenario.

ing). Here again, these observations are valid across realizations (Supplementary Information, Figure S8).

Low Peclet number. The effect of diffusion on the overall transport dynamics for the low Pe case is significant, both in term of arrival time and plume spread. For low degree of heterogeneity ($\sigma_\chi=0.1$), macrodispersion is increased by including diffusion in the simulations (Figure 5, top frame), which is expected and similar to the effect observed in case of a high Pe . However, when σ_χ increases, not including diffusion does not significantly change the early arrivals but prevents late arrival of mass, leading to a non-

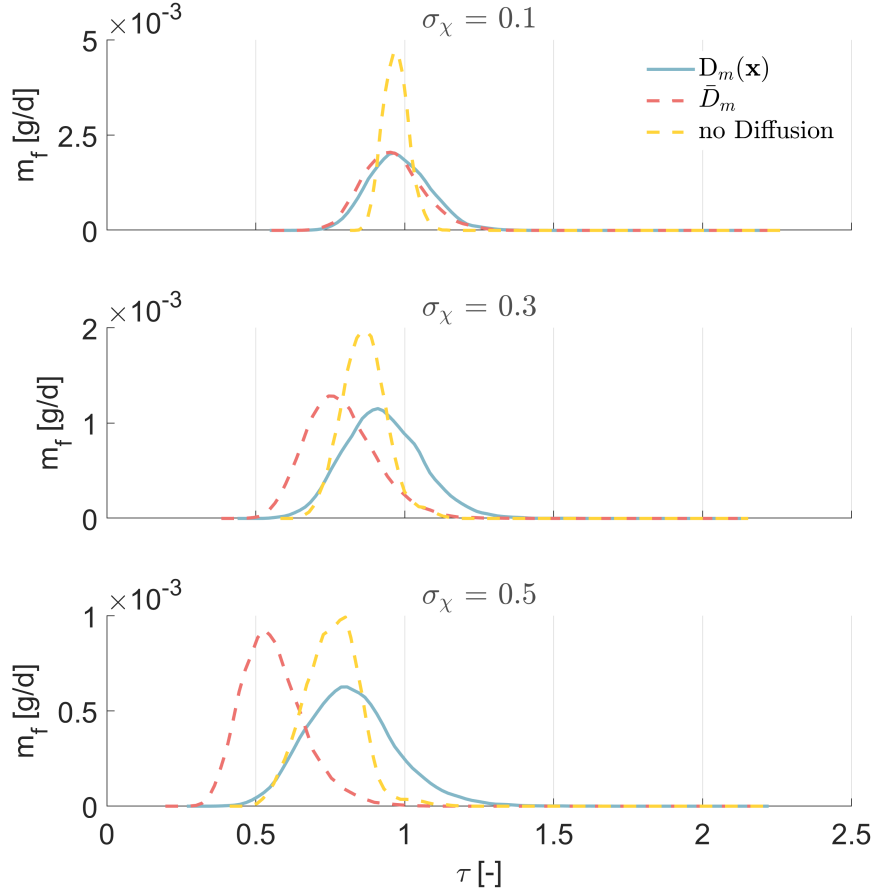


Figure 5. Breakthrough curves (BTCs) resulting from simulations using a spatially variable, tortuosity-dependent diffusion coefficient ($D_m(x)$), a spatially averaged diffusion coefficient (\bar{D}_m) and no diffusion, for soils of different degree of heterogeneity. Results are shown for the lower Peclet number. Times are normalized by the characteristic advective time of the $D_m(x)$ scenario.

Gaussian, negatively skewed BTC (Figure 5, lower frame). BTCs appears then to be more sensitive to Pe as the degree of heterogeneity increases.

At the same time, BTCs sensitivity to σ_χ is specific to the Pe number. When σ_χ increases, the counter-intuitive macrodispersion-reducing effect of diffusion observed for high Pe is not observed for a lower Pe , which disagrees with the previous works of Nisan & Berkowitz (2019); Cirpka & Kitanidis (2002); Weissmann et al. (2002). This relates with our consideration of spatial variable diffusion process. In case of high $q_{z,in}$, low velocity zones are characterized by high diffusion coefficients ($> 10^0 \text{ cm}^2/\text{d}$; Figure 6 lower frame). This is because these zones are characterized by close to saturation

water content but low hydraulic conductivity. This favors the mobilizing of mass that would be otherwise trapped in a system without diffusion, due to the low local velocities. Late arrivals are then prevented. Due to the tortuosity model, the opposite is observed in case of low flux: diffusion values in quasi-stagnant zones are the lowest ($< 10^{-3}$ cm²/d; Figure 6 upper frame), due to the low local water content. Residence times in low velocity zones can then remain relatively high, which allows late arrivals. Interestingly, in a low velocity system without diffusion, mass reaching a fast channel is likely to remain in high velocity zones for the remaining of its transport toward the bottom of the domain. Transport occurs then predominantly in fast channels, reducing the importance of late arrivals. Adding diffusion would favor the transfer of mass from these high velocity zones to more stagnant ones, increasing this way the contribution of late arrivals. Such behavior is consistent across realizations (Supplementary Information, Figure S9). Moreover, accounting for a spatially variable saturated water content leads to similar conclusions (Supplementary Information, Figure S10).

3.3 Effect of Spatially Variable Diffusion

To further understand the implications of spatial variability in the diffusion coefficient, we compare BTCs resulting from simulations with a water content dependent diffusion ($D_m(x)$) coefficient (assuming tortuosity model of Millington and Quirk) and with a homogeneous, averaged diffusion (\bar{D}_m).

In our modeling setting, the range of diffusion coefficient for a single realization is highly dependent on the degree of heterogeneity of the SHPs and on the infiltration rate. In case of lower $q_{z,in}$, we obtain exponentially decreasing histograms of D_m values in case of a high degree of heterogeneity, with a range of diffusion coefficient from 0 to 1.2 cm²/d (Figure 7, top frame). The histogram turns more and more Gaussian-like when σ_χ decreases, with a narrowing range of values (from 0 to 0.3 for $\sigma_\chi = 0.1$).

In case of a larger infiltration rate, ranges of $D_m(x)$ values are globally more spread (Figure 7, bottom frame). Histograms are slightly increasing in case of high degree of heterogeneity, and still Gaussian-like for $\sigma_\chi = 0.1$.

Advection dominated scenario For the high Pe scenario, the spatial variability in the diffusion coefficient appears to have no real impact on transport in a mildly heterogeneous soil (Figure 4, top frame, compare blue and red lines). When the spatial vari-

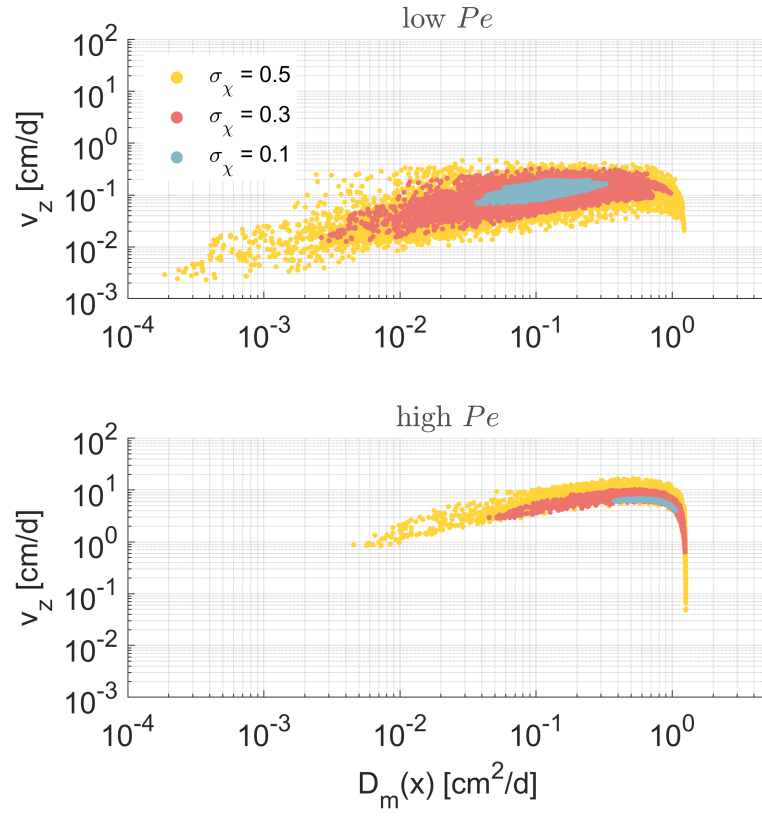


Figure 6. Relationship between the vertical velocity and the water content dependent diffusion coefficient for each degree of the heterogeneity in the soil structure and for the 2 Peclet numbers.

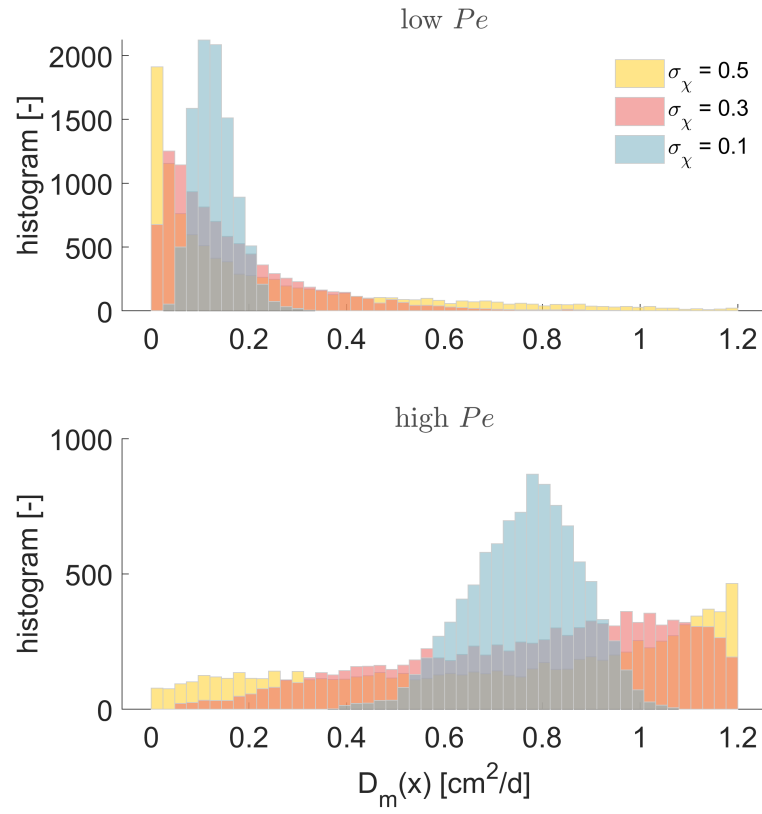


Figure 7. Histograms of the spatially variable, tortuosity-dependent diffusion coefficient for each degree of soil heterogeneity and for a high recharge flux (i.e., high Peclet number; bottom frame) and a low recharge flux (i.e., low Peclet number; top frame).

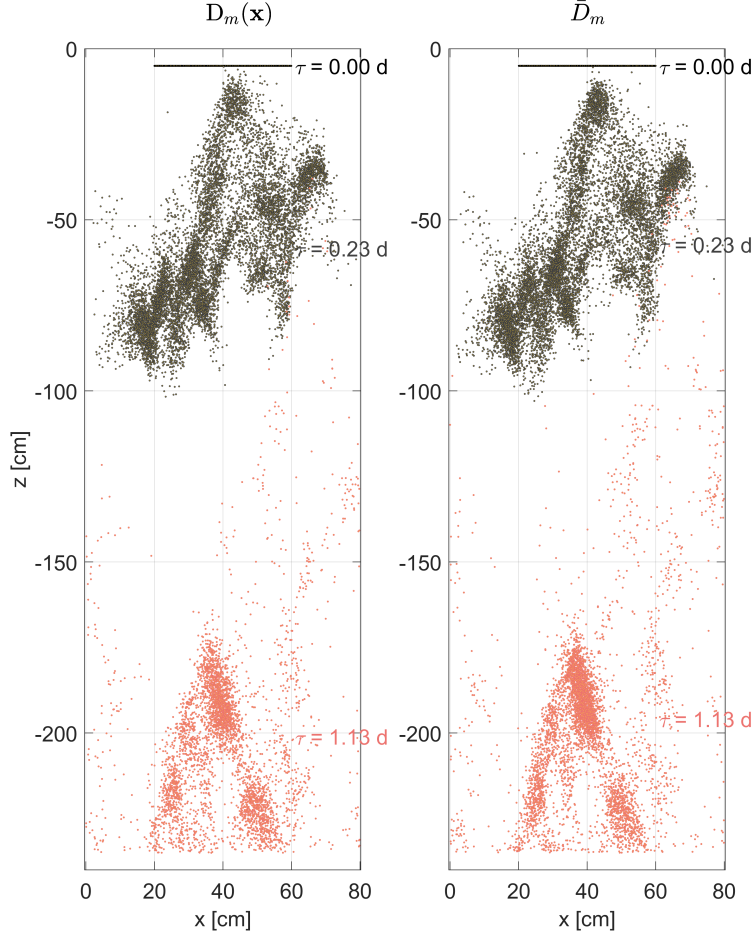


Figure 8. Plume snapshots from simulations using a spatially variable, tortuosity-dependent diffusion coefficient ($D(x)$) and a spatially averaged diffusion coefficient (\bar{D}_m), for soils of a high degree of heterogeneity ($\sigma_\chi = 0.5$). Results are shown for the higher Peclet number.

ability in SHPs is more pronounced, correlating the local diffusion coefficient to the tortuosity (and therefore the water content) slightly decreases the macrodispersion and the tailing of the BTC (Figure 4, bottom frame).

Observing the plume of particles in a highly heterogeneous soil allows to identify zones of accumulation of mass, which is slightly accentuated in case of spatially averaged diffusion coefficient (Figure 8). Globally, the implications in considering the spatial variability in diffusion coefficient for a strongly advective system are moderate. Diffusion coefficients in low velocity zones are higher than the mean values, which, following the previously discussed phenomena, leads to a reduction of late arrivals.

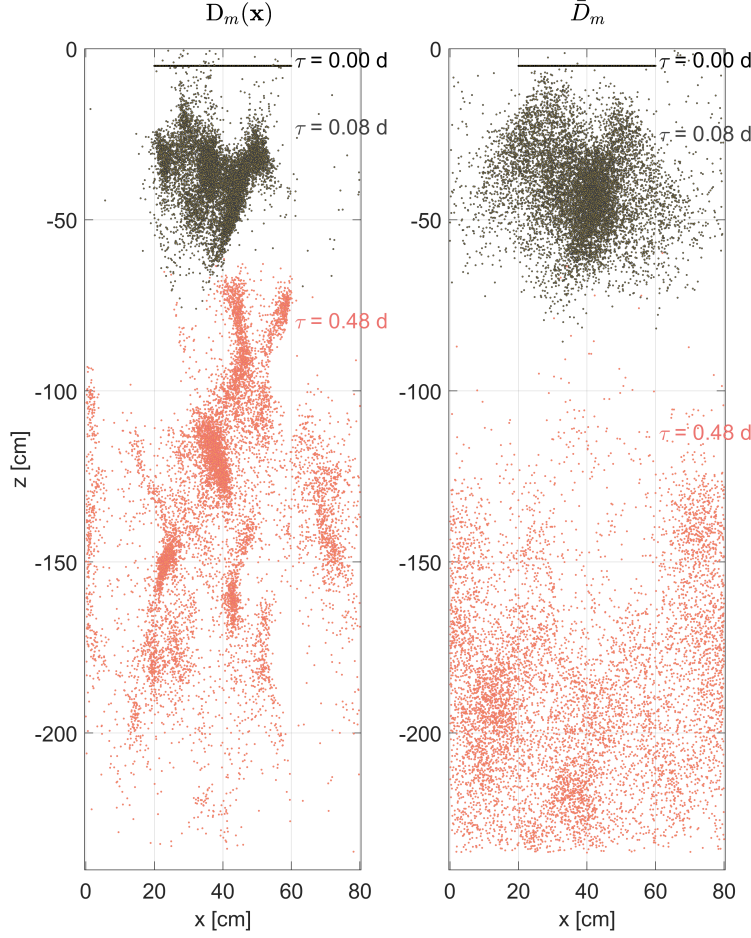


Figure 9. Plume snapshots from simulations using a spatially variable, tortuosity-dependent diffusion coefficient ($D(x)$) and a spatially averaged diffusion coefficient (\bar{D}_m), for soils of a high degree of heterogeneity ($\sigma_\chi = 0.5$). Results are shown for the low Peclet number.

Diffusion dominated scenario. When diffusive process is more dominant, accounting for the spatial variability of the diffusion coefficient has a much greater impact on plume behavior. For a high σ_χ , applying a spatially averaged diffusion coefficient leads to significantly earlier arrival of mass and to a lesser spread of the plume (Figure 5, lower frames).

Snapshots of the particle plume in a highly heterogeneous soil display a significantly pronounced accumulation of mass in specific zones of the soil if diffusion is considered tortuosity-dependent (Figure 9).

Low diffusion coefficient values in low velocity zones result in an increased residence time in those areas, forming pockets of mass, which can only leave the domain at relatively late time. On the other hand, applying an average (but still larger) diffusion coefficient in those low velocity zones allows an earlier mobilization of mass, generating anticipated arrivals. Note that this remains true even compared to a purely advective system, which, despite maintaining mass in fast channels, can still be affected by the relatively long presence of mass in low velocity areas at early times (partly due to the injection of mass in low velocity zones).

3.4 Transient conditions.

Natural systems are characterized by periods of infiltration (i.e., strongly advective flux) and others of mostly slow mass redistribution (i.e., mostly diffusive transport). Figure 10 shows BTCs resulting from simulations with homogeneous and heterogeneous diffusion coefficients, for different distances of the control plane (x_{cp}) and for 2 different durations of the infiltration period ($t_{inf}=1$ day and 15 days). The temporal discretization of fluxes, water contents and diffusion coefficients was set to 1 hour, which produces similar results than for a finer time step (Supplementary Information, Figure S11). The effect of transience in the diffusion process is displayed by comparing BTCs resulting from temporally variable diffusion coefficients (plain lines) and from temporally averaged coefficients (dashed lines). For these 2 cases, the water flux and the water content are still considered transient.

For any infiltration period, results display an insensitivity of the BTCs to the spatial variability in diffusion at the control plane near the source ($x_{cp} = 2 \times \lambda_z$; Figure 10, top frames).

For BTCs recorded near the center of the domain ($x_{cp} = 4 \times \lambda_z$), the spatial variability in the diffusion coefficient generates slightly more diffuse mass arrival, with a later peak and later late arrivals, only if the infiltration period is short (1 day; Figure 10, middle frames). In case of a longer infiltration period (characterized by a strongly advective transport), BTCs at mid-distance are mostly identical for a homogeneous or a heterogeneous diffusion coefficient.

Further downstream ($x_{cp} = 9\lambda_z$), applying a tortuosity-dependent diffusion coefficient produces significantly more diffuse BTCs, with similar early mass arrival than

with a homogeneous D_m , but with a lower peak of mass and later late arrivals (Figure 10, bottom frames). This mass dynamic is observed for both a short (1 day) and a long (15 days) initial period of strongly advective transport. For all tested BTCs, we observed no significant effect of transience in the diffusion coefficient itself.

The two very distinct regimes of diffusive transport associated to a high and a low advective flux explains the main dynamic of the simulated transient transport. At short travel distance, the insensitivity of the solution to the diffusion model can be explained by both the limited sampling of soil heterogeneity occurring over only 2 correlation lengths and by the low impact of spatial variability in diffusion on strongly advective systems. For longer infiltration period, the limited impact of heterogeneity in the diffusion is observed further downstream ($x_{cp} = 2\lambda_z$). Yet, with increased travel distances, the effect of spatially variable diffusion coefficient on strongly diffusive systems takes over, regardless of the infiltration duration.

3.5 Homogenization of diffusion

To evaluate the relevancy in determining effective, homogenized diffusion coefficient other than a spatially averaged values, we tested the performance of the minimum and the maximum values of $D(x)$.

Homogenizing the diffusion coefficient leads to poor performances in case of low Pe systems, regardless of the diffusion coefficient values used (Figure 11, upper frame). Applying the maximum values of diffusion overestimates macrodispersion and leads to early travel times, while the minimum values underestimates the plume spread, despite reproducing relatively well the time of first arrivals.

Thus, no effective, homogenized values of diffusion can be determined in a low Pe system. When velocity is relatively low, zones of low and of high diffusion coefficient have a complex combined effect on transport that evolves as the plume moves through the heterogeneous domain. Therefore, even when the spatial variability in the SPHs, controlling advective fluxes is explicitly described, not accounting for the spatial variability of the diffusion would require to artificially adjust effective advection. Such curve-fitting approach would compromise the physical understanding of the system, which may have detrimental consequences on the applicability of the model.

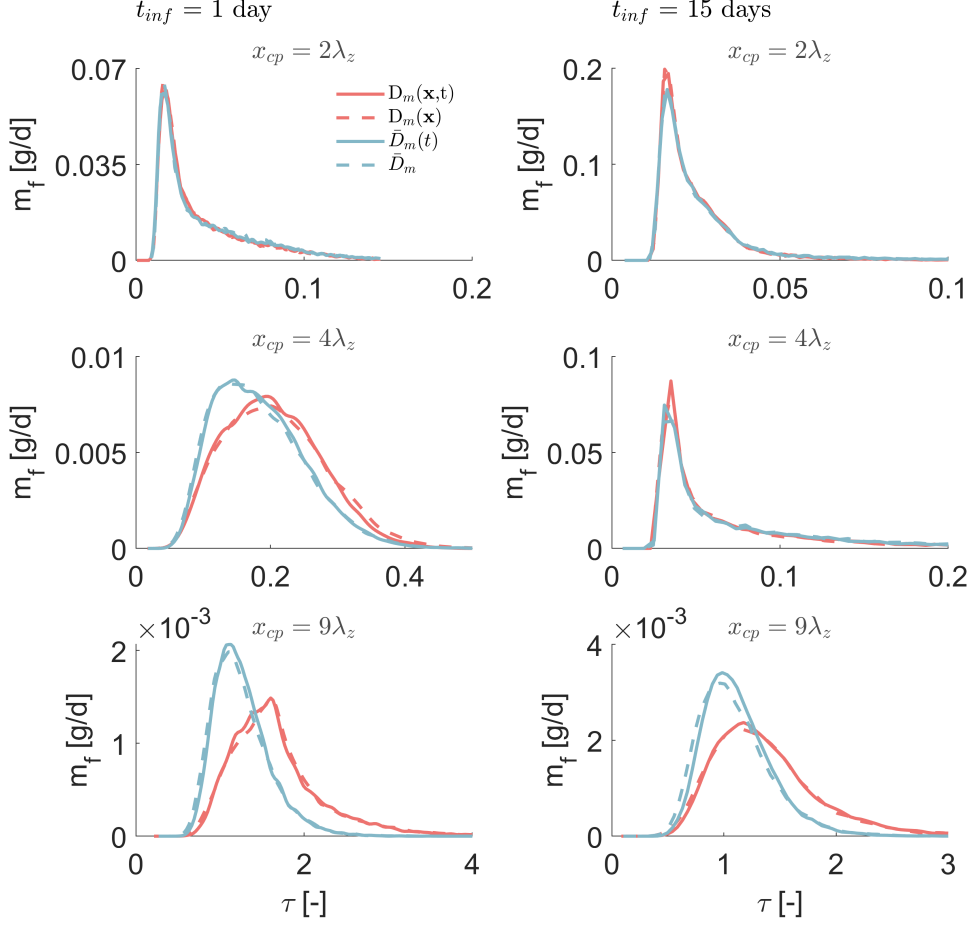


Figure 10. Breakthrough curves (BTCs) at three control planes (CP) resulting from simulations using a spatially variable, tortuosity-dependent diffusion coefficient ($D_m(x)$) and a spatially averaged diffusion coefficient (\bar{D}_m) for 1 day of infiltration (left hand) and 15 days of infiltration (right hand). Diffusion coefficients are considered transient ($D_m(x,t)$ and $\bar{D}_m(t)$) or steady state (temporally averaged). For all simulations, a high degree of heterogeneity in the SHPs ($\sigma_\chi = 0.5$) is considered. Times are normalized by the characteristic advective time estimated for each duration of the infiltration period (t_{inf}).

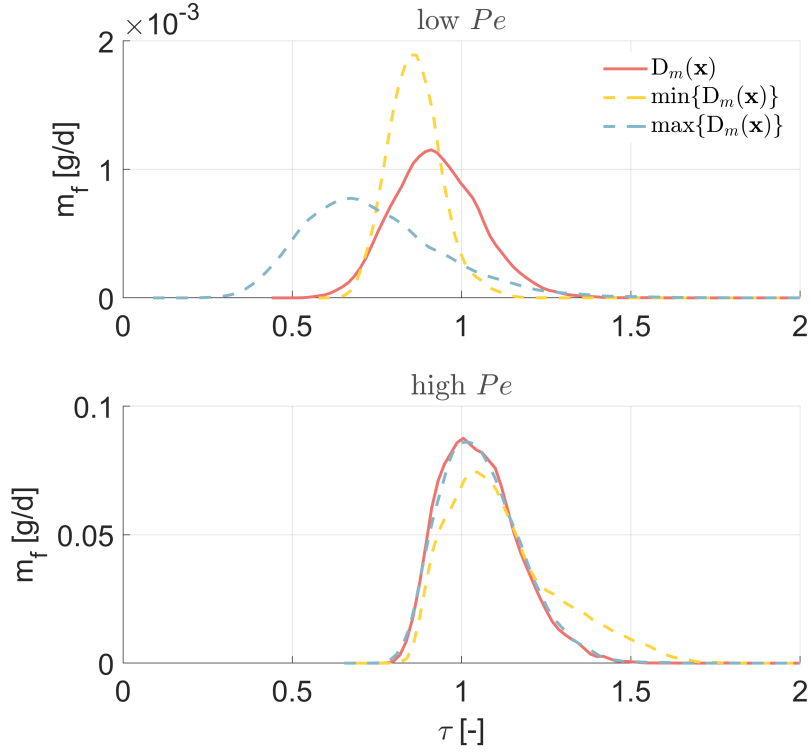


Figure 11. Breakthrough curves (BTCs) resulting from simulations using a spatially variable diffusion coefficient (red plain lines), the minimum (yellow dashed lines) and the maximum (blue dashed lines) values of $D(x)$, for a high recharge flux (bottom frames) and a low recharge flux (top frames). The degree of heterogeneity is described by $\sigma_\chi=0.3$. Times are normalized by the characteristic advective time of the $D_m(x)$ scenario.

In case of high Pe number, a maximum values of $D(x)$ produces satisfactory results, while a minimum values tends to overestimate BTC tailing ((Figure 11, lower frame)). As advection remains the main controlling process, only the zones of high values of diffusion coefficients impact the transport. Maximizing the homogenized diffusion coefficient reproduces then properly the release of mass from low velocity zones that prevent tailing to occur.

4 Concluding remarks

Through a series of numerical simulations, this study analyzed the complex, synergistic effect of (small scale) soil heterogeneity, advection and diffusion on conservative transport in unsaturated soils. Key findings are:

- The control of heterogeneity on transport is Peclet number dependent. For a low Peclet number, the mean advective time increases with the degree of soil heterogeneity, while macrodispersion remains globally unchanged. The opposite is observed for the high Peclet case, which is characterized by a significant increase of (non-Fickian) macrodispersion and no real change in the mean advective flux when soil heterogeneity increases. The sensitivity of high Peclet systems to the degree of soil heterogeneity observed at the pore scale under saturated conditions by Nissan & Berkowitz (2019) remains then valid at larger scale and for unsaturated conditions.
- Diffusion appears to be a key process controlling residence time of solutes in soils since it distributes contaminant mass in or out of low velocity zones. Thus, the impact of diffusion on transport is also highly dependent to the Peclet number, but only for a relatively high degree of heterogeneity. In this case, for a high Peclet number, diffusion decreases macrodispersion by allowing the remobilization of mass trapped in quasi-stagnant zones. This phenomena have been previously described by e.g., Weissmann et al. (2002) for a saturated aquifer and are now also observed for unsaturated conditions. Yet, in a low Peclet system, diffusion increases late arrival of mass. This appears to be linked to the tortuosity dependence of the diffusion coefficient assumed in this study. Unlike for high Peclet systems, our simulated low Peclet soils are characterized by low values of the diffusion coefficient

in low velocity zones (due to the low water saturation value), which prevents the counter-intuitive reduction of macrodispersion when diffusion is considered.

- Thus, the spatial variability in the diffusion process is also a potential significant factor to understand transport behavior of solutes in soils. The impact of tortuosity-dependent diffusion process was found highly dependent on both the degree of heterogeneity and the Peclet number due to (1) the importance that the diffusive process has in regard to the advective flux, and (2) the saturation dependence of the distribution of diffusion coefficients over the soil profile. Homogenizing the diffusion coefficient will disregard the dynamic feedback between mass accumulation in zones of low advective flux and the potential release of this mass, which is function of the magnitude of the local diffusive process. The empirical relationship between local tortuosity and the diffusion coefficient has then important implications in the dynamic of transport.

The practical implications of our theoretical study are potentially important. Indeed, different parametrization of the heterogeneity, velocity and diffusion can lead to significantly different first arrival of mass to the groundwater, more or less long term late arrivals and different peak concentrations reaching soil-connected water bodies. Moreover, natural and cultivated soils are ubiquitously transient systems characterized by important temporal variation in the advection flux. Periods of low and high Peclet numbers due to infiltration or irrigation will result in periods of Fickian and non-Fickian transport characterized with significantly different mean advective velocity and effective dispersion. The flow condition at the moment of field or laboratory observations is therefore a key element to be considered to understand in depth the dynamic of the solute plume. This possible complex control of soil heterogeneity, Peclet number and diffusion on transport is expected to critically affect reaction and reactive transport, which remains to be investigated.

Globally, our outputs clearly highlight that small scale heterogeneity in soils and its overall impact on the spatial variability in diffusion must be considered to properly predict transport. Yet, a detailed characterization of this spatial variability is in most cases technically and economically infeasible. Upscaling approaches reproducing this complex impact of heterogeneity on advection, diffusion and therefore hydraulic structure are then required. Upscaling the effect of heterogeneity on *advective* fluxes has been the

focus on an important effort, mostly in saturated aquifers. Techniques such as the Multi-Rate Mass Transfer model (Haggerty & Gorelick, 1995), Continuous Time Random Walk (Berkowitz et al., 2006), and the fractional Advection-Dispersion Equation (Benson et al., 2000) have indeed been developed to reproduce late arrival times, which is typically the main BTC feature characterizing non-Fickian transport in saturated media. Yet, our work shows that both the heterogeneous advective flux and diffusive flux should be simultaneously upscaled in soils. Indeed, as our results display, (1) a simple homogenization of the diffusion coefficient is not sufficient due to the complex and dynamic mass transfer from and into zones of low velocities, and (2) temporal variations in fluxes conditions the effective impact of diffusion on transport. Guo et al. (2019) exposed the difficulties of upscaling techniques to perform well under transient conditions, which the authors attempted to solve later on by explicitly accounting for the advective flux dependence of mass transfer coefficients (Guo et al., 2020). In a future study, one could attempt to develop a similar approach for unsaturated soils, accounting for both transient advective fluxes and transient diffusive fluxes.

To finish, it is important to emphasize on the theoretical and incomplete nature of this work. For instance, real soils are in more cases more heterogeneous than what has been assumed in this study (biopores, cracks, hydrophobicity, etc). Moreover, our conclusions rely on the application of a series of (well established) equations but also on an empirical relationship between diffusion and tortuosity. While this relation is based on observations, its impact on transport under heterogeneous conditions remains to also be validated by in-situ or laboratory observations.

Open Research Section

This study is theoretical by nature and does not utilize any known database. Instead, model parameters are listed throughout the manuscript. Flow simulations can be reproduced using the Daisy model (Hansen et al., 2012; Holbak et al., 2022) available at: <https://daisy.ku.dk/download/>. Transport simulations can be reproduced using the code RW3D (Henri & Diamantopoulos, 2022). Its source files and an executable are available at: <https://doi.org/10.5281/zenodo.6607599>.

Acknowledgments

The authors gratefully acknowledge the financial support through the Research Executive Agency of the European Commission, Grant Agreement number: 896470.

References

- Bear, J. (1972). *Dynamics of Fluids in Porous Media*. New York: American Elsevier Publishing Company. (764 p.)
- Benson, D. A., Wheatcraft, S. W., & Meerschaert, M. M. (2000). The fractional-order governing equation of lévy motion. *Water Resources Research*, 36(6), 1413-1423. Retrieved from <https://agupubs.onlinelibrary.wiley.com/doi/abs/10.1029/2000WR900032> doi: <https://doi.org/10.1029/2000WR900032>
- Berkowitz, B., Cortis, A., Dentz, M., & Scher, H. (2006). Modeling non-fickian transport in geological formations as a continuous time random walk. *Reviews of Geophysics*, 44(2). Retrieved from <https://agupubs.onlinelibrary.wiley.com/doi/abs/10.1029/2005RG000178> doi: <https://doi.org/10.1029/2005RG000178>
- Botros, F. E., Onsoy, Y. S., Ginn, T. R., & Harter, T. (2012, nov). Richards Equation-Based Modeling to Estimate Flow and Nitrate Transport in a Deep Alluvial Vadose Zone. *Vadose Zone Journal*, 11(4), vzj2011.0145. Retrieved from <http://doi.wiley.com/10.2136/vzj2011.0145> doi: 10.2136/vzj2011.0145
- Boudreau, B. P. (1996). The diffusive tortuosity of fine-grained unlithified sediments. *Geochimica et Cosmochimica Acta*, 60(16), 3139-3142. Retrieved from <https://www.sciencedirect.com/science/article/pii/0016703796001585> doi: [https://doi.org/10.1016/0016-7037\(96\)00158-5](https://doi.org/10.1016/0016-7037(96)00158-5)
- Bromly, M., & Hinz, C. (2004). Non-fickian transport in homogeneous unsaturated repacked sand. *Water Resources Research*, 40(7). Retrieved from <https://agupubs.onlinelibrary.wiley.com/doi/abs/10.1029/2003WR002579> doi: <https://doi.org/10.1029/2003WR002579>
- Cirpka, O. A., & Kitanidis, P. K. (2002). Numerical evaluation of solute dispersion and dilution in unsaturated heterogeneous media. *Water Resources Research*, 38(11), 2-1-2-15. doi: 10.1029/2001wr001262
- Cremer, C. J., Neuweiler, I., Bechtold, M., & Vanderborght, J. (2016, jun). Solute Transport in Heterogeneous Soil with Time-Dependent Boundary Condi-

- tions. *Vadose Zone Journal*, 15(6), vzj2015.11.0144. Retrieved from <http://doi.wiley.com/10.2136/vzj2015.11.0144> doi: 10.2136/vzj2015.11.0144
- Cremer, C. J. M., & Neuweiler, I. (2019, dec). How Dynamic Boundary Conditions Induce Solute Trapping and Quasi-stagnant Zones in Laboratory Experiments Comprising Unsaturated Heterogeneous Porous Media. *Water Resources Research*, 55(12), 10765–10780. Retrieved from <https://onlinelibrary.wiley.com/doi/10.1029/2018WR024470> doi: 10.1029/2018WR024470
- Cushman, J. H. (1984). On unifying the concepts of scale, instrumentation, and stochastics in the development of multiphase transport theory. *Water Resources Research*, 20(11), 1668-1676. Retrieved from <https://agupubs.onlinelibrary.wiley.com/doi/abs/10.1029/WR020i011p01668> doi: <https://doi.org/10.1029/WR020i011p01668>
- Diamantopoulos, E., & Durner, W. (2012). Dynamic nonequilibrium of water flow in porous media: A review. *Vadose Zone J.*, 11(0).
- Fernández-García, D., Illangasekare, T. H., & Rajaram, H. (2005). Differences in the scale-dependence of dispersivity estimated from temporal and spatial moments in chemically and physically heterogeneous porous media. *Adv. Water Res.*, 28(7), 745-759.
- Forrer, I., Kasteel, R., Flury, M., & Flühler, H. (1999, oct). Longitudinal and lateral dispersion in an unsaturated field soil. *Water Resources Research*, 35(10), 3049–3060. Retrieved from <http://doi.wiley.com/10.1029/1999WR900185> doi: 10.1029/1999WR900185
- Ghanbarian, B., Hunt, A. G., Ewing, R. P., & Sahimi, M. (2013). Tortuosity in Porous Media: A Critical Review. *Soil Science Society of America Journal*, 77(5), 1461–1477. doi: 10.2136/sssaj2012.0435
- Guo, Z., Fogg, G. E., Brusseau, M. L., LaBolle, E. M., & Lopez, J. (2019). Modeling groundwater contaminant transport in the presence of large heterogeneity: a case study comparing mt3d and rwhet. *Hydrogeology Journal*, 27(4), 1363–1371. Retrieved from <https://doi.org/10.1007/s10040-019-01938-9> doi: 10.1007/s10040-019-01938-9
- Guo, Z., Henri, C. V., Fogg, G. E., Zhang, Y., & Zheng, C. (2020). Adaptive multirate mass transfer (ammt) model: A new approach to upscale regional-scale transport under transient flow conditions. *Water Resources Research*, 56(2),

- e2019WR026000. Retrieved from <https://agupubs.onlinelibrary.wiley.com/doi/abs/10.1029/2019WR026000> doi: <https://doi.org/10.1029/2019WR026000>
- Haggerty, R., & Gorelick, S. M. (1995). Multiple-rate mass transfer for modeling diffusion and surface reactions in media with pore-scale heterogeneity. *Water Resources Research*, 31(10), 2383–2400. Retrieved from <https://agupubs.onlinelibrary.wiley.com/doi/abs/10.1029/95WR10583> doi: <https://doi.org/10.1029/95WR10583>
- Hammel, K., & Roth, K. (1998, apr). Approximation of asymptotic dispersivity of conservative solute in unsaturated heterogeneous media with steady state flow. *Water Resources Research*, 34(4), 709–715. Retrieved from <http://doi.wiley.com/10.1029/98WR00004> doi: 10.1029/98WR00004
- Hansen, B., Dalgaard, T., Thorling, L., Sørensen, B., & Erlandsen, M. (2012). Regional analysis of groundwater nitrate concentrations and trends in denmark in regard to agricultural influence. *Biogeosciences*, 9, 3277–3286.
- Henri, C. V., & Diamantopoulos, E. (2022). Unsaturated transport modeling: Random-walk particle-tracking as a numerical-dispersion free and efficient alternative to eulerian methods. *Journal of Advances in Modeling Earth Systems*, 14(9), e2021MS002812. Retrieved from <https://agupubs.onlinelibrary.wiley.com/doi/abs/10.1029/2021MS002812> (e2021MS002812 2021MS002812) doi: <https://doi.org/10.1029/2021MS002812>
- Henri, C. V., & Fernàndez-Garcia, D. (2014). Toward efficiency in heterogeneous multispecies reactive transport modeling: A particle-tracking solution for first-order network reactions. *Water Resour. Res.*, 50(9), 7206–7230.
- Henri, C. V., & Fernàndez-Garcia, D. (2015). A random walk solution for modeling solute transport with network reactions and multi-rate mass transfer in heterogeneous systems: Impact of biofilms. *Adv.in Water Resour.*, 86, 119.
- Holbak, M., Abrahamsen, P., & Diamantopoulos, E. (2022). Modeling preferential water flow and pesticide leaching to drainpipes: The effect of drain-connecting and matrix-terminating biopores. *Water Resources Research*, 58(7), e2021WR031608.
- Holbak, M., Abrahamsen, P., Hansen, S., & Diamantopoulos, E. (2021). A physically based model for preferential water flow and solute transport in drained agricultural fields. *Water Resources Research*, 57(3), e2020WR027954.
- Jarvis, N., Koestel, J., & Larsbo, M. (2016). Understanding preferential flow in the

- 676 vadose zone: Recent advances and future prospects. *Vadose Zone Journal*, 15(12),
677 1–11.
- 678 Javaux, M., Vanderborght, J., Kasteel, R., & Vanclooster, M. (2006a). Three-
679 dimensional modeling of the scale-and flow rate-dependency of dispersion in a
680 heterogeneous unsaturated sandy monolith. *Vadose Zone Journal*, 5(2), 515–528.
- 681 Javaux, M., Vanderborght, J., Kasteel, R., & Vanclooster, M. (2006b, may). Three-
682 Dimensional Modeling of the Scale- and Flow Rate-Dependency of Dispersion
683 in a Heterogeneous Unsaturated Sandy Monolith. *Vadose Zone Journal*, 5(2),
684 515–528. Retrieved from <http://doi.wiley.com/10.2136/vzj2005.0056> doi:
685 10.2136/vzj2005.0056
- 686 Khan, A. U.-H., & Jury, W. A. (1990). A laboratory study of the dispersion scale
687 effect in column outflow experiments. *Journal of Contaminant Hydrology*, 5(2),
688 119–131.
- 689 Miller, E., & Miller, R. (1956). Physical theory for capillary flow phenomena. *Jour-
690 nal of Applied Physics*, 27(4), 324–332.
- 691 Millington, R. J., & Quirk, J. P. (1961). Permeability of porous solids. *Transactions
692 of the Faraday Society*, 57, 1200. Retrieved from [http://xlink.rsc.org/?DOI=](http://xlink.rsc.org/?DOI=tf9615701200)
693 [tf9615701200](http://xlink.rsc.org/?DOI=tf9615701200) doi: 10.1039/tf9615701200
- 694 Møldrup, P., Olesen, T., Rolston, D., & Yamaguchi, T. (1997). Modeling diffusion
695 and reaction in soils: Vii. predicting gas and ion diffusivity in undisturbed and
696 sieved soils. *Soil Science*, 162(9), 632–640.
- 697 Nissan, A., & Berkowitz, B. (2019, mar). Anomalous transport dependence on
698 Péclet number, porous medium heterogeneity, and a temporally varying velocity
699 field. *Physical Review E*, 99(3), 033108. Retrieved from [https://link.aps.org/](https://link.aps.org/doi/10.1103/PhysRevE.99.033108)
700 [doi/10.1103/PhysRevE.99.033108](https://link.aps.org/doi/10.1103/PhysRevE.99.033108) doi: 10.1103/PhysRevE.99.033108
- 701 Richards, L. A. (1931). Capillary conduction of liquids through porous mediums.
702 *Journal of Applied Physics*, 1(5), 318–333.
- 703 Richardson, L. F. (1922). *Weather prediction by numerical process*. New York: Cam-
704 bridge University Press. (Cambridge: Cambridge mathematical library)
- 705 Roth, K. (1995, sep). Steady State Flow in an Unsaturated, Two-Dimensional,
706 Macroscopically Homogeneous, Miller-Similar Medium. *Water Resources Research*,
707 31(9), 2127–2140. Retrieved from <http://doi.wiley.com/10.1029/95WR00946>
708 doi: 10.1029/95WR00946

- Roth, K., & Hammel, K. (1996, jun). Transport of conservative chemical through an unsaturated two-dimensional Miller-similar medium with steady state flow. *Water Resources Research*, 32(6), 1653–1663. Retrieved from <http://doi.wiley.com/10.1029/96WR00756> doi: 10.1029/96WR00756
- Russo, D. (1993). Stochastic modeling of macrodispersion for solute transport in a heterogeneous unsaturated porous formation. *Water Resources Research*, 29(2), 383–397. Retrieved from <https://agupubs.onlinelibrary.wiley.com/doi/abs/10.1029/92WR01957> doi: <https://doi.org/10.1029/92WR01957>
- Russo, D. (2015, may). On the effect of connectivity on solute transport in spatially heterogeneous combined unsaturated-saturated flow systems. *Water Resources Research*, 51(5), 3525–3542. Retrieved from <http://doi.wiley.com/10.1002/2014WR016434> doi: 10.1002/2014WR016434
- Russo, D., & Fiori, A. (2009, mar). Stochastic analysis of transport in a combined heterogeneous vadose zone-groundwater flow system. *Water Resources Research*, 45(3), 1–16. Retrieved from <http://doi.wiley.com/10.1029/2008WR007157> doi: 10.1029/2008WR007157
- Russo, D., Zaidel, J., & Laufer, A. (2000). Numerical analysis of flow and transport in a combined heterogeneous vadose zone-groundwater system. *Advances in Water Resources*, 24(1), 49–62. doi: 10.1016/S0309-1708(00)00026-9
- Russo, D., Zaidel, J., & Laufer, A. (2001, aug). Numerical analysis of flow and transport in variably saturated bimodal heterogeneous porous media. *Water Resources Research*, 37(8), 2127–2141. Retrieved from <http://doi.wiley.com/10.1029/2001WR000393> doi: 10.1029/2001WR000393
- Sadeghi, M., Ghahraman, B., Warrick, A. W., Tuller, M., & Jones, S. B. (2016). A critical evaluation of the miller and miller similar media theory for application to natural soils. *Water Resources Research*, 52(5), 3829–3846.
- Schelle, H., Durner, W., Schlüter, S., Vogel, H.-J., & Vanderborght, J. (2013). Virtual soils: Moisture measurements and their interpretation by inverse modeling. *Vadose Zone Journal*, 12(3), 1–12.
- Schlüter, S., Vanderborght, J., & Vogel, H. J. (2012). Hydraulic non-equilibrium during infiltration induced by structural connectivity. *Advances in Water Resources*, 44, 101–112. doi: 10.1016/j.advwatres.2012.05.002
- Shen, L., & Chen, Z. (2007). Critical review of the impact of tortuosity on diffusion.

- 742 *Chemical Engineering Science*, 62(14), 3748-3755. Retrieved from [https://www](https://www.sciencedirect.com/science/article/pii/S0009250907003144)
 743 [.sciencedirect.com/science/article/pii/S0009250907003144](https://www.sciencedirect.com/science/article/pii/S0009250907003144) doi: [https://](https://doi.org/10.1016/j.ces.2007.03.041)
 744 doi.org/10.1016/j.ces.2007.03.041
- 745 Ursino, N., & Gimmi, T. (2004). Combined effect of heterogeneity, anisotropy
 746 and saturation on steady state flow and transport: Structure recognition
 747 and numerical simulation. *Water Resources Research*, 40(1), 1–12. doi:
 748 10.1029/2003WR002180
- 749 Van Cappellen, P., & Gaillard, J.-F. (2018). Biogeochemical dynamics in aquatic
 750 sediments. In *Reactive transport in porous media* (pp. 335–376). De Gruyter.
- 751 Vanderborght, J., Mallants, D., & Feyen, J. (1998, dec). Solute transport in a
 752 heterogeneous soil for boundary and initial conditions: Evaluation of first-order
 753 approximations. *Water Resources Research*, 34(12), 3255–3270. Retrieved from
 754 <http://doi.wiley.com/10.1029/98WR02685> doi: 10.1029/98WR02685
- 755 Van Genuchten, M., & Wierenga, P. (1974). *Simulation of one-dimensional solute*
 756 *transfer in porous media*. New Mexico State University, Agricultural Experiment
 757 Station. Retrieved from <https://books.google.dk/books?id=kxInAQAAMAAJ>
- 758 Vogel, T., Gerke, H. H., Zhang, R., & Van Genuchten, M. T. (2000). Model-
 759 ing flow and transport in a two-dimensional dual-permeability system with spa-
 760 tially variable hydraulic properties. *Journal of Hydrology*, 238(1-2), 78–89. doi:
 761 10.1016/S0022-1694(00)00327-9
- 762 Šimunek, J., Šejna, M., Saito, H., Sakai, M., & Van Genuchten, M. (2013). The
 763 hydrus-1d software package for simulating the movement of water, heat, and mul-
 764 tiple solutes in variably saturated media, version 4.17, hydrus software series 3,
 765 department of environmental sciences, university of california riverside, riverside,
 766 california. USA.
- 767 Weissmann, G. S., Zhang, Y., LaBolle, E. M., & Fogg, G. E. (2002). Dispersion of
 768 groundwater age in an alluvial aquifer system. *Water Resour. Res.*, 38(10), 1198.
- 769 Woods, S. A., Dyck, M. F., & Kachanoski, R. G. (2013, may). Spatial and tem-
 770 poral variability of soil horizons and long-term solute transport under semi-
 771 arid conditions. *Canadian Journal of Soil Science*, 93(2), 173–191. Retrieved
 772 from <http://www.nrcresearchpress.com/doi/10.4141/cjss2012-082> doi:
 773 10.4141/cjss2012-082